Structural insight into the substrate specificity of Bombyx mori β-fructofuranosidase belonging to the glycoside hydrolase family 32

Structural insight into the substrate specificity of *Bombyx mori* β-fructofuranosidase belonging to the glycoside hydrolase family 32

Takatsugu Miyazaki[1,2*], Nozomi Oba[2], and Enoch Y. Park[1,2]

[1] Green Chemistry Research Division, Research Institute of Green Science and Technology, Shizuoka University, 836 Ohya, Suruga-ku, Shizuoka, 422-8529, Japan.

[2] Department of Applied Life Sciences, Faculty of Agriculture, Shizuoka University, 836 Ohya, Suruga-ku, Shizuoka, 422-8529, Japan.

***Correspondence:** Takatsugu Miyazaki, Green Chemistry Research Division, Research Institute of Green Science and Technology, Shizuoka University, 836 Ohya, Suruga-ku, Shizuoka, 422-8529, Japan; Tel: +81-54-238-4886; E-mail: miyazaki.takatsugu@shizuoka.ac.jp

Running Title: Structure of *B. mori* GH32 β-fructofuranosidase

Abstract

Sucrose-hydrolyzing enzymes are largely divided into β-fructofuranosidase and sucrose α-glucosidase. The domestic silkworm *Bombyx mori* possesses both enzymes, BmSUC1 and BmSUH, belonging to the glycoside hydrolase family 32 (GH32) and GH13, respectively. BmSUC1 was presumed to be acquired by horizontal gene transfer from bacteria based on phylogenetic analysis and related to tolerance to sugar-mimic alkaloids contained in mulberry latex. Here we investigated the substrate specificity of recombinant BmSUC1 that can hydrolyze not only sucrose but also fructooligosaccharides and fructans, and revealed that the enzyme was competitively inhibited by 1,4-dideoxy-1,4-imino-D-arabinitol, one of the alkaloids. Moreover, the crystal structures of BmSUC1 in apo form and complex with sucrose were determined, and the active site pocket was shallow and suitable for shorter substrates but was related to more relaxed substrate specificity than the strict sucrose α-glucosidase BmSUH. Considering together with the distribution of BmSUC1-orthologous genes in many lepidopterans, our results suggest that BmSUC1 contributes to the digestion of fructooligosaccharides and fructans derived from feed plants.

Keywords: *Bombyx mori*, sucrose, β-fructofuranosidase, glycoside hydrolase family 32, crystal structure, 1,4-dideoxy-1,4-imino-D-arabinitol

Abbreviations: BlFFase, *Bifidobacterium longum* β-fructofuranosidase; DAB, 1,4-dideoxy-1,4-imino-D-arabinitol; DNJ, 1-deoxynojirimycin; GH, glycoside hydrolase; HGT, horizontal gene transfer; PDB, Protein Data Bank; SoFFase, *Schwaniomyces occidentalis* β-fructofuranosidase; TmFFase, *Thermotoga maritima* β-fructofuranosidase

1. Introduction

Sucrose is a widely distributed disaccharide, which is one of the main products of photosynthesis used as a carbon source by many organisms. This disaccharide is generally hydrolyzed by glycoside hydrolases (GHs) to produce glucose and fructose, which are primary substrates for glycolysis (Reid and Abratt, 2005; Ruan, 2014). GHs acting on sucrose are divided into two types based on their mechanism. One is β-fructofuranosidase (also known as invertase, EC 3.2.1.26), which recognizes a β-fructofuranosyl residue and hydrolyzes sucrose *via* a covalent fructosyl-enzyme intermediate (Lammens et al., 2009); the other one is sucrose α-glucosidase (also called sucrase, EC 3.2.1.48) recognizes an α-glucopyranosyl residue and hydrolyzes the α-glucosidic linkages of sucrose (Sim et al., 2010). β-Fructofuranosidases, which are mainly found in bacteria, fungi, and plants, belong to GH32 and GH68 families based on their amino acid sequence homology according to the CAZy database (http://www.cazy.org) (Lombard et al., 2014). These families form the clan GH-J and share the five-bladed β-propeller fold of catalytic domains with the same catalytic machinery (Lammens et al., 2009). On the other hand, sucrases are identified as GH13 from bacteria and insects, GH31 from mammals, and GH100 from bacteria and plants.

The domestic silkworm *Bombyx mori* possesses two sucrose-hydrolyzing enzymes, BmSUC1 and BmSUH, belonging to GH32 and GH13 subfamily 17 (GH13_17), respectively. BmSUC1 is a secreted enzyme expressed in the midgut and silk glands (Daimon et al., 2008); BmSUH is a membrane-associated enzyme expressed in the midgut and is a major sucrose hydrolase in the lepidopteran species (Wang et al., 2015). GH32 proteins are rarely observed in the animal kingdom, and especially, mammals do not possess GH32 enzymes. However, genes encoding GH32 proteins were reportedly found in only the genomes of Lepidoptera and Coleoptera among insects (Daimon et al., 2008; Pedezzi et al., 2014; Zhao et al., 2014). Phylogenetic analyses indicated that their genes were acquired *via* horizontal gene transfer (HGT) events from bacteria. *B. mori* possesses two GH32 genes, *BmSUC1* and *BmSUC2*, the latter of which encodes an inactive protein where the catalytic nucleophile residue is mutated (Daimon et al., 2008). Latex of mulberry, which is the sole feed of *B. mori*, contains high concentrations of sugar-mimic alkaloids such as 1-deoxynojirimycin (DNJ) and

1,4-dideoxy-1,4-imino-D-arabinitol (DAB) (Fig. 1), which are glycosidase inhibitors (Konno et al., 2006). These compounds are harmless to *B. mori* because BmSUC1 is not inhibited by DNJ, and BmSUH is inhibited by DNJ and DAB but less sensitive than GH13_17 sucrose hydrolases from other lepidopterans (Daimon et al., 2008; Wang et al., 2015).

We recently determined the crystal structure of GH13_17 BmSUH and revealed the mechanisms of sucrose-specific hydrolysis and inhibition by DNJ and DAB (Miyazaki and Park, 2020). Both compounds competitively inhibited BmSUH with K_i values in the micromolar level and were bound to its active site in their complex structures. However, the relationship between these enzymes and tolerance to these alkaloids and why *B. mori* possesses two sucrose-hydrolyzing enzymes remain unclear. In this study, we examined the substrate specificity toward several β-fructofuranosides and crystal structures of the other isozyme BmSUC1. Combined with biochemical examination, the complex structure with sucrose showed the structure–function relationship in BmSUC1. The results provide novel insights into the substrate recognition mechanism and the physiological function of insect β-fructofuranosidases.

2. Materials and methods

2.1. Materials and strains

Sucrose, 1-kestose, nystose, and raffinose were purchased from FUJIFILM Wako Pure Chemical Co. (Osaka, Japan). 1-Deoxynojirimycin and 1,4-dideoxy-1,4-imino-D-arabinitol were purchased from Carbosynth (Compton, Berkshire, UK). Levan from *Erwinia herbicola* and inulin from dahlia tubers (molecular weight, ~5,000) were obtained from Merck (Darmstadt, Germany) and Nacalai Tesque (Osaka, Japan), respectively. Figure 1 describes the chemical structures of substrates and inhibitors used in this study. All other chemicals were reagent grade and obtained from standard commercial sources. *Escherichia coli* strains DH5α and BL21 (DE3) were used for DNA manipulation and protein expression, respectively.

2.2. Cloning, expression, purification, and mutagenesis

First-strand cDNA was synthesized by reverse transcription with total RNA from fifth-instar larvae (Ehime Sanshu, Ehime, Japan) as described previously (Miyazaki et al., 2019). A signal peptide of BmSUC1 was predicted by the SignalP server (http://www.cbs.dtu.dk/services/SignalP/). A DNA fragment coding BmSUC1 without the signal sequence (Met1–Ala21) was amplified by PCR using cDNA as a template, KOD-Plus-Neo DNA polymerase (Toyobo, Osaka, Japan), and a pair of primers, 5'-TTT TCA TAT GCT CCG CCA GCA AAA TGA GAC-3' and 5'-TTT TAA GCT TAA GCG GGT ACA CTT CTT CTC-3' (restriction sites are underlined). The resultant DNA was digested with NdeI and HindIII (New England Biolabs, Ipswich, MA) and ligated into a pET-28a vector (Merck), followed by DNA sequencing. The nucleotide sequence of *BmSUC1* was submitted to DDBJ/EMBL/GenBank under the accession number LC542934. The recombinant protein had an N-terminal His-tag and a thrombin-cleavage site (MGSSHHHHHHSSGLVPRGSHM-) prior to Leu22. Site-directed mutagenesis was performed using PCR with the expression plasmid as a template and desired primers: 5'-ATG AAT GCC CCT AAC GGC TTT TCA TAC-3' (sense) and 5'-GTT AGG GGC ATT CAT CCA GCC GAC GGG C-3' (anti-sense) for D63A; and 5'-ATG TGG GCA TGT CCC GAT CTG TTT GAA C-3' (sense) and 5'-GGG ACA TGC CCA CAT GTA GCC CAT GTC G-3' (anti-sense) for E234A.

E. coli BL21 (DE3) harboring desired plasmids was grown at 37°C in 1 L LB medium containing 50 μg/mL kanamycin. When the culture reached an optical density of 0.6–0.8 measured at 600 nm, it was induced with isopropyl-β-D-thiogalactopyranoside at a final concentration of 0.1 mM and further incubated for about 20 h at 20°C. Cells were harvested by centrifugation at 10,000 × g for 5 min and resuspended in 50 mM sodium phosphate buffer (pH 8.0) containing 20 mM imidazole and 300 mM NaCl before disruption by sonication. The cell lysate was centrifuged at 20,000 × g for 20 min to remove insoluble materials. The supernatant was applied to a nickel (Ni^{2+}) nitrilotriacetic acid (Ni-NTA) agarose (Qiagen, Hilden, Germany) column equilibrated with the same buffer. The column was washed with buffer, and recombinant proteins were eluted with 50 mM sodium phosphate buffer (pH 8.0) containing 250 mM imidazole and 300 mM NaCl. Fractions containing active enzymes were concentrated using Amicon Ultra 30,000 molecular weight cut-off (Merck) and further purified by gel filtration chromatography using an ÄKTA explorer system with a Superdex

200 Increase 10/300 column (GE Healthcare) and 20 mM sodium phosphate buffer (pH 7.0) containing 300 mM NaCl. Protein purity was confirmed by SDS-PAGE (Supplementary Fig. S1). The protein concentration was determined by absorbance at 280 nm based on theoretical molar absorption coefficients (126,740 M^{-1} cm^{-1}) calculated using the ExPASy ProtParam server (http://web.expasy.org/protparam/).

2.3. Enzyme assays

All activity assays were performed at 30°C in 50 mM HEPES-NaOH buffer (pH 7.0), and reactions were initiated by adding an appropriate amount of enzyme and were quenched by boiling for 10 min. For kinetic parameter determination, at least seven concentrations of substrates were used: 0.25–50 mM sucrose, 0.25–20 mM raffinose, 0.1–20 mM 1-kestose and nystose, 2.5–20 mg/mL inulin and levan. The enzyme concentrations used were 1 μg/mL (17.9 nM) for sucrose and raffinose, and 10 μg/mL (179 nM) for the other substrates. For sucrose hydrolysis, the amount of liberated glucose was quantified using the glucose oxidase–peroxidase method with a Glucose C-II Test Kit (Wako Pure Chemicals, Osaka, Japan). The amount of reducing sugar released after hydrolysis of other substrates, except for sucrose was quantified using the Somogyi–Nelson methods (Somogyi, 1952). Kinetic parameters were calculated by fitting to the Michaelis–Menten equation using nonlinear regression analysis by KaleidaGraph software (Synergy Software, Reading PA, USA). For the inhibition kinetic assay for inhibitors, the same reaction mixtures supplemented with each inhibitor were used, and the inhibition constant was calculated according to a competitive inhibition model.

2.4. Structural analysis

Proteins (25 mg/mL) were crystallized at 20°C using the hanging-drop vapor diffusion method, in which 1.0 μL of protein solution was mixed with an equal volume of a crystallization reservoir solution. Initial crystallization screening was performed using Crystal Screen, Crystal Screen 2, PEG/Ion Screen, and PEG/Ion 2 Screen kits (Hampton Research, Aliso Viejo, CA, USA). Well-diffracted BmSUC1 crystals were obtained by microseeding with a crystallization solution containing 13%–20% (w/v) polyethylene glycol 3,350 (Hampton Research), 40 mM citric acid, and 60 mM 1,3-bis[tris(hydroxymethyl)methylamino]propane.

Before the X-ray diffraction data collection, crystals were cryoprotected with the reservoir solution supplemented with 20% (v/v) ethylene glycol (for unliganded) or 30% (w/v) sucrose (for sucrose complex) and then flash-frozen in liquid nitrogen.

Diffraction data were collected at the BL5A beamline (Photon Factory, Tsukuba, Japan). All data were processed using XDS (Kabsch, 2010). Initial solutions were obtained using the automated molecular replacement program MrBUMP (Keegan and Winn, 2007). The best solution was obtained when *Thermotoga maritima* β-fructofuranosidase (Protein Data Bank entry, 1UYP) was used as a search model. Refinement and manual model building were performed using REFMAC5 (Murshudov et al., 1997) and COOT (Emsley et al., 2010), respectively. Solvent molecules were introduced using ARP/wARP (Carolan and Lamzin, 2014). Structure validation was performed using MolProbity (Williams et al., 2018). Coordinates and structural factors were deposited in the Worldwide Protein Data Bank (http://wwpdb.org/). Structural similarity searches were conducted using the Dali server (Holm, 2019). Computational docking between BmSUC1 and DAB was performed using AutoDock 4.2.6 (Morris et al., 2009). Figures were prepared using PyMOL (Schrödinger LLC, New York, NY, USA).

2.5. Sequence alignment and phylogenetics

Protein sequences were obtained from NCBI Protein database (https://www.ncbi.nlm.nih.gov/protein/) and PSI-BLAST search (https://blast.ncbi.nlm.nih.gov/Blast.cgi) with BmSUC1 as a query. The primary sequence alignment was performed using ClustalOmega (Sievers and Higgins, 2018). Alignment figures were generated by ESPript 3.0 (Robert and Gouet, 2014). For the phylogenetic analysis of GH32 proteins, the sequences were aligned using MUSCLE (Edgar, 2004), and then the phylogenetic analysis was performed using the maximum likelihood method conducted by MEGA X (Kumar et al., 2018). The phylogenetic tree was visualized using the iTOL v5 server (https://itol.embl.de/) (Letunic and Bork, 2019).

3. Results

3.1. Substrate specificity of recombinant BmSUC1

The recombinant BmSUC1 without the N-terminal signal peptide was expressed in *E. coli*, yielding approximately 18 mg per liter culture. Because only sucrose and raffinose have been tested for BmSUC1 hydrolytic activity, we investigated whether the enzyme could hydrolyze other fructooligosaccharides and fructans (Fig. 1). The recombinant enzyme efficiently hydrolyzed sucrose and raffinose with almost identical catalytic efficiency, as reported previously (Daimon et al., 2008), whereas 1-kestose and nystose were hydrolyzed with lower efficiency (Table 1). The isozyme GH13_17 BmSUH has a higher k_{cat}/K_m value than BmSUC1 toward sucrose but lower than 2% activity toward Fruβ(2↔1)αGlc linkage of 1-kestose and nystose (Miyazaki and Park, 2020). BmSUC1 also showed hydrolytic activity toward inulin and levan, which contain β(2→1)- and β(2→6)-fructosidic linkages, respectively. Although individual K_m values could not be determined due to the limit of polysaccharide solubility, the k_{cat}/K_m toward levan slightly exceeded that of inulin. These results indicate that BmSUC1 has a wide substrate specificity and can hydrolyze fructooligosaccharides and fructans compared with BmSUH, which is specific for sucrose.

The substrate specificity of GH32 β-fructofuranosidases from different sources vary widely: β-fructofuranosidase from *Thermotoga maritima* (TmFFase, sequence identity with BmSUC1 = 34%) was reported to hydrolyze sucrose better than raffinose and inulin (Liebl et al., 1998); β-fructofuranosidase from *Bifidobacterium longum* (BlFFase, 33%) preferred longer fructooligosaccharides, 1-kestose, and nystose to sucrose and hydrolyzed inulin (Bujacz et al., 2011); β-fructofuranosidase from *Schwaniomyces occidentalis* yeast (SoFFase, 25%) also hydrolyzed nystose more efficiently than sucrose (Alvaro-Benito et al., 2010). Among them, BmSUC1 preferred shorter oligosaccharides to longer fructooligosaccharides and polysaccharides.

3.2. Overall structure

The crystal structure of BmSUC1 was determined at 1.8 Å resolution by the molecular replacement method using the coordinate of TmFFase (PDB entry 1UYP) (Alberto et al., 2004). The crystal belongs to the space group $C222_1$ containing one molecule in the

asymmetric unit (Table 2). BmSUC1 comprises largely two domains, an N-terminal five-bladed β-propeller catalytic domain (residues 47–350) and a C-terminal β-sandwich domain (357–488) (Fig. 2A). An α-helix (25–46) is located at the N-terminus before the catalytic domain, and a short α-helical linker (351–356) is located between the catalytic and C-terminal domains. A structural homology search using the Dali server revealed that high *Z* scores were observed for TmFFase (PDB entry 1UYP; *Z* = 48.0; Alberto et al., 2004), *Lactobacillus gasseri* putative sucrose-6-phosphate hydrolase (PDB entry 6NU8; *Z* = 45.8; unpublished), *Bifidobacterium adolescentis* putative β-fructofuranosidase (PDB entry 6NUN; *Z* = 45.7; unpublished), and BlFFase (PDB entry 3PIG; *Z* = 45.1; Bujacz et al., 2011), which are bacterial GH32 enzymes with 27%–34% amino acid sequence identities to BmSUC1. In contrast, the most structurally homologous enzyme among the structure-determined eukaryotic GH32 proteins is endo-inulinase Inu2 from a fungus *Aspergillus ficuum* (PDB entry 3SC7; *Z* = 40.8; Pouyez et al., 2012). The N-terminal β-propeller domain and the C-terminal β-sandwich domain are completely conserved among GH32 enzymes. The superimposition of the whole structure of BmSUC1 and the reported GH32 β-fructofuranosidases demonstrates that the main chain of BmSUC1 is almost identical to those of the other β-fructofuranosidases, except for several loops (Fig. 2B). Also, the N-terminal α-helical region of unknown function is conserved among only BlFFase and some bacterial GH32 proteins (PDB entry 6NU8 and 6NUN) but not in the other reported GH32 enzymes, including the structure-determined eukaryotic GH32 enzymes. These characteristics support the hypothesis that the gene for ancestral protein of BmSUC1 was derived from bacteria.

3.3. Active site of BmSUC1 complexed with substrate

To obtain the complex structure with the substrate, we constructed the mutants D63A and E234A, where the nucleophilic Asp and acid/base Glu residues, respectively, were substituted with Ala. Both mutants lost the hydrolytic activity toward sucrose (below 0.2% of wild-type activity). We performed soaking and cocrystallization experiments, and the D63A crystal soaked with sucrose was diffracted to 1.9 Å resolution. An electron density map for sucrose was observed at the center of the β-propeller catalytic domain (Fig. 3A and B). The fructose

residue (Fru −1) of sucrose interacts with nine amino acid residues (side chains of Asn62, Asp63, Gln79, Trp87, Met90, Ser119, Arg180, Asp181, Glu234, and Trp317, and the main chain of Ser119) *via* hydrogen bonds (Fig. 3C and Supplementary Table S1). In contrast, the glucose residue (Glc +1) of sucrose forms a hydrogen bond with Glu234 and Gln252 and interacts with Trp87 and Trp317 by hydrophobic interaction. The amino acid residues interacting with Fru −1 are well conserved in GH32 β-fructofuranosidases but the residues surrounding Glc +1 are not (Fig. 4).

The active site of TmFFase in complex with raffinose (PDB entry 1W2T) was superimposed into BmSUC1 active site (Fig. 3D). Although the amino acid residues of subsites −1 and +1 are almost conserved between these enzymes, residues surrounding galactose residue (Gal +2) of raffinose at subsite +2 differ slightly. Gal +2 hydrophobically interacts with Trp41, and its corresponding residue is conserved as Trp87 in BmSUC1 as well as other β-fructofuranosidases (Figs. 3D and 4). The side chain of Arg136 is located in the vicinity of the O6 group of Gal +2, suggesting that Arg136 is probably involved in recognizing Gal +2. This residue is substituted to Tyr92 in TmFFase and not conserved in other β-fructofuranosidases.

3.4. Inhibition of BmSUC1 hydrolysis by sugar-mimic alkaloids

BmSUC1 was reported to be insensitive to DNJ and DAB, but there are no data on DAB in the literature (Daimon et al., 2008). Because the stereochemistry of DAB resembles that of fructofuranose (Fig. 1), we investigated BmSUC1 activity with various concentrations of DAB and DNJ. BmSUC1 activity toward sucrose was reduced to 3% with 50 mM DAB, whereas BmSUC1 retained 76% activity with the same concentration of DNJ (Fig. 5A). The activity decreased to less than half when 1 mM DAB was added, indicating that BmSUC1 was more sensitive to DAB than DNJ. The kinetic assays revealed that the inhibitory mechanism of DAB was competitive and K_i value was 800 μM (Fig. 5B). The K_i values of DAB and DNJ toward BmSUH were 4.2 and 290 μM, respectively (Miyazaki and Park, 2020), indicating that BmSUC1 was less sensitive to the sugar-mimic alkaloids contained in mulberry latex than BmSUH.

The model of DAB was docked into BmSUC active site using AutoDock. The DAB

model was located at subsite −1, although the orientation of its ring differed from the fructofuranoside of sucrose (Fig. 5C). DAB was predicted to form hydrogen bonds with Asn62, Gln79, Trp87, Asp181, and the catalytic acid/base Asp234. Because DAB is furanose-mimic and smaller than pyranose-mimic DNJ, it was possible that DAB could enter the subsite −1 and be bound tightly but DNJ could not.

4. Discussion

This study unveiled the three-dimensional structure of BmSUC1 using X-ray crystallography. The entire structure of BmSUC1 resembles those of bacterial GH32 β-fructofuranosidases rather than the structure-determined eukaryotic GH32 β-fructofuranosidases, which agrees with their sequence homology. Despite the similarity in the overall folding and the subsite −1 structure to the structure-determined GH32 β-fructofuranosidases, the conformation of a loop (Loop-A, residues 136–147) in the vicinity of the catalytic site differed from the corresponding loops in bacterial and fungal β-fructofuranosidases (Figs. 2B and 6). The catalytic pocket of BmSUC1 is shallow and the number of residues forming subsites +1 and +2 is fewer than that of subsite −1 like TmFFase. In contrast, BlFFase prefers longer substrates, 1-kestose and nystose, to sucrose and its corresponding loop is slightly longer than BmSUC1 and TmFFase (Figs. 4 and 6). The loop of BlFFase gets inside and forms a part of the catalytic pocket, probably to cause longer substrate preference. The corresponding loop of eukaryotic SoFFase, which is also good at longer substrates, is shorter than BmSUC1 but its dimeric counterpart forms plus subsites and enables it to bind longer substrates instead (Alvaro-Benito et al., 2012). Collectively, BmSUC1 has the structural feature that determines its wide substrate specificity that sucrose and raffinose are main substrates but longer fructooligosaccharides and fructans can be substrates with lower efficiency.

HGT has been recognized as a key event for evolution in various organisms, including bacteria and archaea with multicellular eukaryotes (Soucy et al., 2015; Husnik and McCutcheon, 2018). Studies of genes that were transferred from bacteria to insects that contribute to their adaptation have been reported (Husnik et al., 2013; Gusev et al., 2014; Wybouw et al., 2016). Bacteria-to-insect HGTs of GHs have also been considered: *e.g.*

cellulases (Pauchet et al., 2014; Busch et al., 2019), hemicellulases (Acuna, 2012; Pauchet and Heckel, 2013), polygalacturonases (Pauchet et al., 2010a; Kirsch et al., 2014; Pauchet et al, 2014), and chitinase (Daimon et al., 2003). Most of these GHs are involved in degrading plant cell wall polysaccharides while *B. mori* chitinase BmChi-h plays a critical role in chitin cuticle degradation during the molting process (Daimon et al., 2005). BmSUC1 was identified as a gene transferred from bacteria and initially thought to contribute to tolerance toward sugar-mimic alkaloids that are contained in diet mulberry leaves (Daimon et al., 2008). However, recombinant BmSUC1 was enzymatically revealed to be inhibited by DAB in this study. Mulberry leaves and the sugar-mimic alkaloids remarkably inhibited the growth of polyphagous lepidopterans *Samia ricini* and *Mamestra brassicae* but not *B. mori* (Konno et al., 2006). Moreover, sucrose-hydrolyzing activity in the membrane and soluble fractions of *S. ricini* midgut was inhibited by DNJ and DAB, while that in *B. mori* midgut was not (IC_{50} > 1 mM) (Hirayama et al., 2007). Although the concentration of the alkaloids reportedly reached 1.5%–2.5% (8%–18% dry weight), it is quantitatively unclear whether the concentration of these compounds directly affects sucrose-hydrolyzing enzymes in the midgut of lepidopterans after taking in mulberry leaves. Other factors are probably involved in alkaloid tolerance although further investigation is required.

B. mori was domesticated more than 5000 years ago from the wild progenitor *Bombyx mandarina*. Recent genome projects have analyzed the genome sequences of various lepidopterans, including *B. mandarina* (Xiang et al., 2018), revealing that many lepidopterans possess genes for GH32 proteins. A sequence homology search using PSI-BLAST found numerous GH32 sequences from both Lepidoptera and other classes such as Coleoptera, Diptera, Hemiptera, and Thysanoptera. Lepidopteran GH32 genes have been identified to express in the midgut by transcriptomic and proteomic analyses (Pauchet et al., 2008; Pauchet et al., 2010b), and beetle GH32 genes also expressed in the midgut (Pedezzi et al., 2014; Zhao et al., 2014), suggesting that insect GH32 β-fructofuranosidases with BmSUC1 also contribute to the digestion of sucrose in their midguts. This is supported by a multiple sequence alignment showing that the residues involved in the hydrolysis and substrate recognition are almost conserved between BmSUC1 and insect GH32 proteins (Supplementary Fig. S2). Lepidopteran GH32 proteins classified into the same clade as

BmSUC1 seem to share a common ancestor, and most of these lepidopterans have genes for GH13_17 sucrose hydrolases like *B. mori* (Miyazaki and Park, 2020). Why do lepidopterans possess two sucrose-hydrolyzing enzymes? As described above, BmSUC1 was found to exhibit the hydrolytic activity toward fructooligosaccharides and fructans in addition to sucrose and raffinose, which were also previously reported as substrates (Daimon et al., 2008). 1-Kestose, nystose, and inulin are produced by GH32 fructosyltransferases in many plants (Lammens et al., 2009). One possibility is that herbivorous lepidopterans can digest these carbohydrates more efficiently using GH32 orthologs in addition to GH13_17 SUH orthologs. The knockdown of *BmSUC1* delayed larval development and reduced body size, indicating that BmSUC1 plays a critical role in carbohydrate digestion (Gan et al., 2018). 1-Kestose was identified in *B. mori* larval hemolymph, suggesting that BmSUC1 has transglycosylation activity although its physiological significance is unclear (Gan et al., 2018).

In conclusion, we extensively investigated BmSUC1 substrate specificity and determined its three-dimensional structures in the apo form and in complex with the substrate. BmSUC1 exhibited wide substrate specificity to hydrolyze both sucrose and longer β-fructofuranosides. The active site structure is related to the relaxed substrate specificity, and the enzyme and lepidopteran orthologs may play a crucial role in the digestion of fructooligosaccharides and fructans derived from their feed plants.

Acknowledgments

We thank the staff of the Photon Factory for their help in X-ray data collection. This research was performed under the approval of the Photon Factory Program Advisory Committee (Proposal No. 2019G097). This work was supported in part by the Japan Society for the Promotion of Science KAKENHI (grant No. 19K15748). We thank Enago (www.enago.jp) for the English language review.

Data availability

The nucleotide sequence of BmSUC1 cloned in this study has been deposited in the DDBJ/EMBL/GenBank database under the accession number LC542934. The atomic coordinates and structure factors for BmSUC1 and D63A complexed with sucrose (PDB ID

7BWB and 7BWC) have been deposited in the worldwide Protein Data Bank.

Author contributions

TM conceived and supervised the study; TM and NO performed experiments; TM and EYP analyzed the data; TM wrote and revised the manuscript; All authors approved the manuscript.

Conflict of interest

The authors declare that they have no conflicts of interest with the contents of this article.

References

Acuna, R., 2012. Adaptive horizontal transfer of a bacterial gene to an invasive insect pest of coffee. Proc. Natl. Acad. Sci. U. S. A. 109, 4197–4202.

Alberto, F., Bignon, C., Sulzenbacher, G., Henrissat, B., Czjzek, M., 2004. The three-dimensional structure of invertase (β-fructosidase) from *Thermotoga maritima* reveals a bimodular arrangement and an evolutionary relationship between retaining and inverting glycosidases. J. Biol. Chem. 279, 18903–18910.

Alvaro-Benito, M., Polo, A., González, B., Fernández-Lobato, M., Sanz-Aparicio, J., 2010. Structural and kinetic analysis of *Schwanniomyces occidentalis* invertase reveals a new oligomerization pattern and the role of its supplementary domain in substrate binding. J. Biol. Chem. 285, 13930–13941.

Álvaro-Benito, M., Sainz-Polo, M. A., González-Pérez, D., González, B., Plou, F. J., Fernández-Lobato, M., Sanz-Aparicio, J., 2012. Structural and kinetic insights reveal that the amino acid pair Gln-228/Asn-254 modulates the transfructosylating specificity of *Schwanniomyces occidentalis* β-fructofuranosidase, an enzyme that produces prebiotics. J. Biol. Chem. 287, 19674–19686.

Bujacz, A., Jedrzejczak-Krzepkowska, M., Bielecki, S., Redzynia, I., Bujacz, G., 2011. Crystal structures of the apo form of β-fructofuranosidase from *Bifidobacterium longum* and its complex with fructose. FEBS J. 278, 1728–1744.

Busch, A., Danchin, E. G. J., Pauchet, Y., 2019. Functional diversification of horizontally acquired glycoside hydrolase family 45 (GH45) proteins in *Phytophaga* beetles. BMC Evol. Biol. 19, 100.

Carolan, C. G., Lamzin, V. S., 2014. Automated identification of crystallographic ligands using sparse-density representations. Acta Crystallogr. D Biol. Crystallogr. 70, 1844–1853.

Daimon, T., Hamada, K., Mita, K., Okano, K., Suzuki, M. G., Kobayashi, M., Shimada, T., 2003. A *Bombyx mori* gene, *BmChi-h*, encodes a protein homologous to bacterial and baculovirus chitinases. Insect Biochem. Mol. Biol., 33, 749–759.

Daimon, T., Katsuma, S., Iwanaga, M., Kang, W., Shimada, T., 2005. The *BmChi-h* gene, a bacterial-type chitinase gene of *Bombyx mori*, encodes a functional exochitinase that plays a role in the chitin degradation during the molting process. Insect Biochem. Mol. Biol. 35, 1112–1123.

Daimon, T., Taguchi, T., Meng, Y., Katsuma, S., Mita, K., Shimada, T., 2008. β-Fructofuranosidase genes of the silkworm, *Bombyx mori*: insights into enzymatic adaptation of *B. mori* to toxic alkaloids in mulberry latex. J. Biol. Chem. 283, 15271–15279.

Edgar, R. C., 2004. MUSCLE: multiple sequence alignment with high accuracy and high throughput. Nucleic Acids Res. 32, 1792–1797.

Emsley, P., Lohkamp, B., Scott, W. G., Cowtan, K., 2010. Features and development of Coot. Acta Crystallogr. D Biol. Crystallogr. 66, 486–501.

Gan, Q., Zhang, X., Zhang, D., Shi, L., Zhou, Y., Sun, T., Jiang, S., Gao, J., Meng, Y., 2018. BmSUC1 is essential for glycometabolism modulation in the silkworm, *Bombyx mori*. Biochim. Biophys. Acta Gene Regul. Mech. 1861, 543–553.

Gusev, O., Suetsugu, Y., Cornette, R., Kawashima, T., Logacheva. M. D., Kondrashov, A. S., Penin, A. A., Hatanaka, R., Kikuta, S., Shimura, S., Kanamori, H., Katayose, Y., Matsumoto, T., Shagimardanova, E., Alexeev, D., Govorun, V., Wisecaver, J., Mikheyev, A., Koyanagi, R., Fujie, M., Nishiyama, T., Shigenobu, S., Shibata, T. F., Golygina, V., Hasebe, M., Okuda, T., Satoh, N., Kikawada, T., 2014. Comparative genome sequencing reveals genomic signature of extreme desiccation tolerance in the anhydrobiotic midge. Nat. Commun. 5, 4784.

Hirayama, C., Konno, K., Wasano, N., Nakamura, M., Differential effects of sugar-mimic alkaloids in mulberry latex on sugar metabolism and disaccharidases of Eri and domesticated silkworms: enzymatic adaptation of *Bombyx mori* to mulberry defense. Insect Biochem. Mol. Biol. 37, 1348–1358.

Holm, L., 2019. Benchmarking fold detection by DaliLite v.5. Bioinformatics 35, 5326–5327.

Husnik, F., McCutcheon, J. P., 2018. Functional horizontal gene transfer from bacteria to eukaryotes. Nat. Rev. Microbiol. 16, 67–79.

Husnik, F., Nikoh, N., Koga, R., Ross, L., Duncan, R. P., Fujie, M., Tanaka, M., Satoh, N., Bachtrog, D., Wilson, A. C., von Dohlen, C. D., Fukatsu, T., McCutcheon, J. P., Horizontal gene transfer from diverse bacteria to an insect genome enables a tripartite nested mealybug symbiosis. Cell 153, 1567–1578.

Kabsch, W., 2010. XDS. Acta Crystallogr. D Biol. Crystallogr. 66, 125–132.

Keegan, R. M., Winn, M. D., 2007. Automated search-model discovery and preparation for

464 structure solution by molecular replacement. Acta Crystallogr. D Biol. Crystallogr. 63, 447–
465 457.
466
467 Kirsch, R., Gramzow, L., Theißen, G., Siegfried, B. D., Ffrench-Constant, R. H., Heckel, D.
468 G., Pauchet, Y. 2014. Horizontal gene transfer and functional diversification of plant cell wall
469 degrading polygalacturonases: key events in the evolution of herbivory in beetles. Insect
470 Biochem. Mol. Biol. 52, 33–50.
471
472 Konno, K., Ono, H., Nakamura, M., Tateishi, K., Hirayama, C., Tamura, Y., Hattori, M.,
473 Koyama, A., Kohno, K., 2006. Mulberry latex rich in antidiabetic sugar-mimic alkaloids
474 forces dieting on caterpillars. Proc. Natl. Acad. Sci. U. S. A. 103, 1337–1341.
475
476 Kumar, S., Stecher, G., Li, M., Knyaz, C., Tamura, K., 2018. MEGA X: Molecular
477 Evolutionary Genetics Analysis across Computing Platforms. Mol. Biol. Evol., 35, 1547–
478 1549.
479
480 Lammens, W., Le Roy, K., Schroeven, L., Van Laere, A., Rabijns, A., Van den Ende, W., 2009.
481 Structural insights into glycoside hydrolase family 32 and 68 enzymes: functional
482 implications. J. Exp. Bot. 60, 727–740.
483
484 Letunic, I., Bork, P., 2019. Interactive Tree Of Life (iTOL) v4: recent updates and new
485 developments. Nucleic Acids Res. 47, W256–W259.
486
487 Liebl, W., Brem, D., Gotschlich, A., 1998. Analysis of the gene for β-fructosidase (invertase,
488 inulinase) of the hyperthermophilic bacterium *Thermotoga maritima*, and characterisation of
489 the enzyme expressed in *Escherichia coli*. Appl. Microbiol. Biotechnol. 50, 55–64.
490
491 Lombard, V., Golaconda Ramulu, H., Drula, E., Coutinho, P. M., Henrissat, B., 2014. The
492 carbohydrate-active enzymes database (CAZy) in 2013. Nucleic Acids Res 42, D490–D495.
493

494 Miyazaki, T., Park, E. Y., 2020. Structure–function analysis of silkworm sucrose hydrolase
495 uncovers the mechanism of substrate specificity in GH13 subfamily 17 *exo*-α-glucosidases. J.
496 Biol. Chem. 295, 8784–8797.
497
498 Miyazaki, T., Miyashita, R., Nakamura, S., Ikegaya, M., Kato, T., Park, E. Y., 2019.
499 Biochemical characterization and mutational analysis of silkworm *Bombyx mori*
500 β-1,4-*N*-acetylgalactosaminyltransferase and insight into the substrate specificity of
501 β-1,4-galactosyltransferase family enzymes. Insect Biochem. Mol. Biol. 115, 103254.
502
503 Morris, G. M., Huey, R., Lindstrom, W., Sanner, M. F., Belew, R. K., Goodsell, D. S., Olson,
504 A. J., 2009. Autodock4 and AutoDockTools4: automated docking with selective receptor
505 flexiblity. J. Comput. Chem. 30, 2785–2791.
506
507 Murshudov, G. N., Vagin, A. A., Dodson, E. J., 1997. Refinement of macromolecular
508 structures by the maximum-likelihood method. Acta Crystallogr. D Biol. Crystallogr. 53, 240–
509 255.
510
511 Pauchet, Y., Heckel, D. G., 2013. The genome of the mustard leaf beetle encodes two active
512 xylanases originally acquired from bacteria through horizontal gene transfer. Proc. R. Soc.
513 B-Biol. Sci. 280, 20131021.
514
515 Pauchet, Y., Kirsch, R., Giraud, S., Vogel, H., Heckel, D. G., 2014. Identification and
516 characterization of plant cell wall degrading enzymes from three glycoside hydrolase families
517 in the cerambycid beetle *Apriona japonica*. Insect Biochem. Mol. Biol. 49, 1–13.
518
519 Pauchet, Y., Muck, A., Svatos, A., Heckel, D. G., Preiss, S., 2008. Mapping the larval midgut
520 lumen proteome of *Helicoverpa armigera*, a generalist herbivorous insect. J. Proteome Res. 7,
521 1629–1639.
522
523 Pauchet, Y., Wilkinson, P., Chauhan, R., Ffrench-Constant, R. H., 2010a. Diversity of beetle

genes encoding novel plant cell wall degrading enzymes. PLoS One 5, e15635.

Pauchet, Y., Wilkinson, P., Vogel, H., Nelson, D. R., Reynolds, S. E., Heckel, D. G., Ffrench-Constant, R. H., 2010b. Pyrosequencing the *Manduca sexta* larval midgut transcriptome: messages for digestion, detoxification and defence. Insect Mol. Biol. 19, 61–75.

Pedezzi, R., Fonseca, F. P. P., Santos Júnior, C. D., Kishi, L. T., Terra, W. R., Henrique-Silva, F., 2014. A novel β-fructofuranosidase in Coleoptera: Characterization of a β-fructofuranosidase from the sugarcane weevil, *Sphenophorus levis*. Insect Biochem. Mol. Biol. 55, 31–38.

Pouyez, J., Mayard, A., Vandamme, A. M., Roussel, G., Perpète, E. A., Wouters, J., Housen, I., Michaux, C., 2012. First crystal structure of an endo-inulinase, INU2, from *Aspergillus ficuum*: discovery of an extra-pocket in the catalytic domain responsible for its endo-activity. Biochimie 94, 2423–2430.

Reid, S. J., Abratt, V. R., 2005. Sucrose utilisation in bacteria: genetic organisation and regulation. Appl. Microbiol. Biotechnol. 67, 312–321.

Robert, X., Gouet. P., 2014. Deciphering key features in protein structures with the new ENDscript server. Nucleic Acids Res 42, W320–W324.

Ruan, Y. L., 2014. Sucrose metabolism: gateway to diverse carbon use and sugar signaling. Annu. Rev. Plant Biol. 65, 33–67.

Sievers, F., Higgins, D. G., 2018. Clustal Omega for making accurate alignments of many protein sequences. Protein Sci. 27, 135–145.

554 Sim, L., Willemsma, C., Mohan, S., Naim, H. Y., Pinto, B. M., Rose, D. R., 2010. Structural
555 basis for substrate selectivity in human maltaseglucoamylase and sucrase-isomaltase
556 N-terminal domains. J. Biol. Chem. 285, 17763–17770.
557
558 Somogyi, M., 1952. Notes on sugar determination. J. Biol. Chem. 195, 19–23.
559
560 Soucy, S. M., Huang, J., Gogarten, J. P., 2015. Horizontal gene transfer: building the web of
561 life. Nat. Rev. Genet. 16, 472–482.
562
563 Wang, H., Kiuchi, T., Katsuma, S., Shimada, T., 2015. A novel sucrose hydrolase from the
564 bombycoid silkworms *Bombyx mori*, *Trilocha varians*, and *Samia cynthia ricini* with a
565 substrate specificity for sucrose. Insect Biochem. Mol. Biol. 61, 46–52.
566
567 Williams, C. J., Hintze, B. J., Headd, J. J., Moriarty, N. W., Chen, V. B., Jain, S., Prisant, M.
568 G., Lewis, S. M., Videau, L. L., Keedy, D. A., Deis, L. N., Arendall, W. B. III, Verma, V.,
569 Snoeyink, J. S., Adams, P. D., Lovell, S. C., Richardson, J. S., Richardson, D. C., 2018.
570 MolProbity: More and better reference data for improved all-atom structure validation.
571 Protein Sci. 27, 293–315.
572
573 Wybouw, N., Pauchet, Y., Heckel, D. G., Van Leeuwen, T., 2016. Horizontal gene transfer
574 contributes to the evolution of arthropod herbivory. Genome Biol. Evol. 8, 1785–1801.
575
576 Xiang, H., Liu, X., Li, M., Zhu, Y., Wang, L., Cui, Y., Liu, L., Fang, G., Qian, H., Xu, A.,
577 Wang, W., Zhan, S., 2018. The evolutionary road from wild moth to domestic silkworm. Nat.
578 Ecol. Evol. 2, 1268–1279.
579
580 Zhao, C., Doucet, D., Mittapalli, O., 2014. Characterization of horizontally transferred
581 β-fructofuranosidase (*ScrB*) genes in *Agrilus planipennis*. Insect Mol. Biol. 23, 821–832.
582

583 **Table 1. Activity of β-fructofuranosidases toward β-fructofuranosides.**

Enzyme	Substrate	k_{cat} (s^{-1})	K_m (mM)	k_{cat}/K_m (s^{-1} mM^{-1})	Relative activity (%) [a]	Reference
BmSUC1	Sucrose	97.3 ± 1.5	4.89 ± 0.25	19.8	100	This study
	Raffinose	386 ± 28	18.7 ± 2.4	20.6	104	
	1-Kestose	6.62 ± 0.37	1.08 ± 0.24	6.14	31.0	
	Nystose	6.35 ± 0.55	1.79 ± 0.55	3.55	17.9	
	Inulin	–	–	0.248 [b]	–	
	Levan	–	–	0.295 [b]	–	
TmBfrA	Sucrose	2.6×10^3	64	4.1×10^4	100	Liebl et al., 1998
	Raffinose	1.4×10^2	15	9.3×10^3	22.7	
	Inulin	5.9×10^2	19	3.1×10^4	75.6	
BlFFase	Sucrose	NA [c]	31.5	NA	100	Bujacz et al., 2011
	Raffinose	NA	64.6	NA	6.7	
	1-Kestose	NA	4.74	NA	263	
	Nystose	NA	1.29	NA	128	
	Inulin	NA	8.87	NA	59	
	Levan	NA	NA	NA	0	
SoInv	Sucrose	106	6.4	16.6	100	Alvaro-Benito et al., 2010
	Nystose	84	2.4	35	211	
	Inulin	25	12	2.1	12.6	
BmSUH [d]	Sucrose	41.2	0.92	44.7		Miyazaki and Park, 2020

584 [a]Each k_{cat}/K_m value for sucrose is taken as 100%. For BlFFase, the values reported in Bujacz et al.,
585 2011 are listed.
586 [b]Values (s^{-1} mg^{-1} mL) were estimated from the slope of velocity–substrate concentration plots due to
587 the solubility limit of substrates.
588 [c]NA, not available.
589 [d]*B. mori* sucrase belonging to GH13_17.
590

Table 2. Data collection and refinement statistics.

	WT unliganded	D63A-sucrose complex
Data collection		
Beamline	PF BL5A	PF BL5A
Wavelength (Å)	1.0000	1.0000
Space group	$C222_1$	$C222_1$
Cell dimensions		
a, b, c (Å)	94.8, 119.3, 100.3	96.5, 118.5, 101.3
Resolution range (Å)	50–1.80 (1.90–1.80)	50–1.95 (2.06–1.95)
Measured reflections	318,179	271,920
Unique reflections	52,834	42,574
Completeness (%)	99.9 (99.8)	99.9 (99.9)
Redundancy	6.0 (5.0)	6.4 (6.7)
Mean $I/\sigma(I)$	17.0 (2.5)	13.1 (2.1)
R_{merge}	0.051 (0.607)	0.063 (0.661)
CC1/2	(0.858)	(0.934)
Refinement statistics		
R_{work} / R_{free}	0.168 / 0.213	0.216 / 0.247
RMSD		
Bond lengths (Å)	0.009	0.005
Bond angles (°)	1.523	1.315
Number of atoms		
Protein	3,784	3,786
Sucrose	-	23
Water	188	144
Average *B* (Å^2)		
Protein	43.1	54.8
Ligands	-	64.9
Water	35.5	45.6
Ramachandran plot		
Favored (%)	95.7	94.8
Outliers (%)	0.2	0.2
PDB codes	7BWB	7BWC

The values for the highest resolution shells are given in parentheses.

Figure legends

Figure 1. Substrates and inhibitors.

Figure 2. Structure of BmSUC1.

(A) Ribbon representation of the overall structure of BmSUC1. Colors are as follows: N-terminal region (residues 25–46), *gray*; catalytic domain (47–350), *rainbow* (from *blue* to *red*); linker (351–356), *white*; C-terminal domain (357–488), *purple*. Five blades (I–V) of the catalytic domain are indicated. Nt and Ct mean the N and C termini, respectively. **(B)** Structural comparison with GH32 β-fructofuranosidases. Colors used are as follows: BmSUC1, *red*; TmFFase, *blue*; BlFFase, *yellow*; SoFFase, *cyan*. Arrow indicates Loop-A (136–147) in blade II.

Figure 3. Active site of BmSUC1 D63A complexed with sucrose. (A) F_o−F_c omit electron density map contoured at 3.3 σ and modeled sucrose are shown as *blue mesh* and *pink stick*, respectively. **(B)** The sucrose molecule (*pink stick*) bound to the active site of BmSUC1 D63A (*gray*). **(C)** Stereo view of the active site. The side chains of amino acid residues interacting with sucrose and the main chain of Ser119 are shown in *green stick* models, and the catalytic residues and sucrose are in *cyan* and *pink*, respectively. Hydrogen bonds are represented by *dashed lines*. The catalytic nucleophile Asp63 in the WT apo structure is superimposed. Nuc and A/B in parentheses mean nucleophilic and acid/base catalysts, respectively. **(D)** Superposition of BmSUC1 D63A complexed with sucrose and TmFFase E190D complexed with raffinose (PDB entry 1W2T) in stereo. Colors used are as follows: BmSUC1, *green*; catalytic Asp63 and Glu234, *cyan*; sucrose, *pink* (*thin stick*); TmFFase, *slate blue*; raffinose, *magenta*.

Figure 4. Multiple sequence alignment of GH32 β-fructofuranosidases. The sequences of BmSUC1 and the structure-known GH32 β-fructofuranosidases, BlFFase (GenBank ABN04092.1), TmFFase (AAD36485.1), and SoFFase (ADN34605.1) were aligned using Clustal Omega and the figure generated by ESPript 3.0. Secondary structures and domain

architecture of BmSUC1 are described above sequences and colors for the domains are the same as Fig. 2A. The predicted signal sequences of BmSUC1 and SoFFase are underlined with *dashed* lines. Loop-A and the corresponding regions are boxed with *dotted* lines. The catalytic residues and residues interacting with sucrose in BmSUC1 are highlighted in *cyan* and *green*, respectively. Their identical residues in the other β-fructofuranosidases are also highlighted in the same colors.

Figure 5. Inhibition of BmSUC1 hydrolysis. (A) Relative activity of BmSUC1 toward sucrose (10 mM) with various concentrations of DNJ (*filled circle*) and DAB (*filled square*). **(B)** Double reciprocal plots of BmSUC1 activity toward sucrose without (*open square*) and with 0.5 mM (*gray square*) or 1.0 mM (*filled square*) DAB. **(C)** Molecular docking of DAB into BmSUC1. The molecular surface of BmSUC1 is shown in *gray* with transparency. The side chains of the catalytic residues and other active site residues are shown in *cyan* and *green stick* models, respectively. The docked DAB and sucrose in D63A-sucrose are in *brown* and *thin pink* sticks, respectively. Predicted hydrogen bonds between DAB and BmSUC1 are indicated as *dashed lines.*

Figure 6. Structural comparison of active sites of GH32 β-fructofuranosidases. The active sites of BmSUC1 **(A)**, BlFFase in complex with fructose (*yellow stick*) **(B)**, TmFFase E190D mutant in complex with raffinose (*magenta stick*) **(C)**, and SoFFase D50A mutant in complex with inulin (*slate blue stick*) **(D)** are shown as molecular surface models. In **(A)**, sucrose (*pink stick*) molecule of D63A-sucrose is superimposed, and the other ligands in **(B–D)** are also superimposed and shown as *thin stick* models. **(A–D)** Loop-A (Arg136–Glu147) of BmSUC1 and the corresponding regions are shown in *green* and the dimeric counterpart of SoFFase is shown in *wheat*. Sugar-binding subsites are indicated in parenthesis.

Fig. 1 Miyazaki et al.

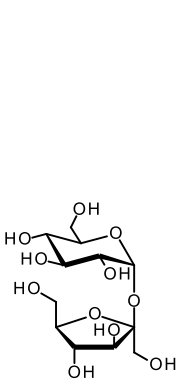

sucrose

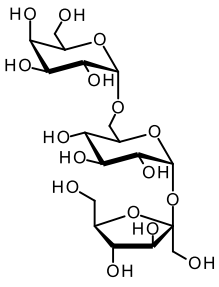

raffinose

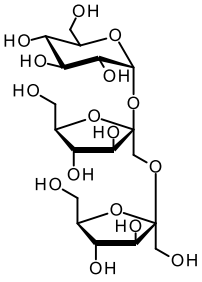

1-kestose

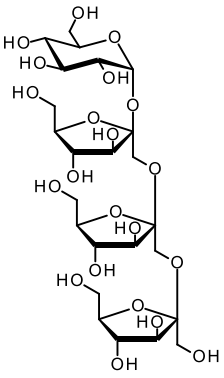

nystose

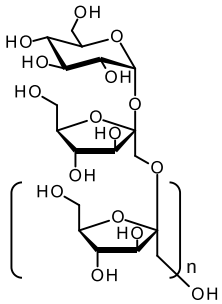

inulin

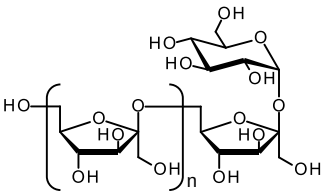

levan

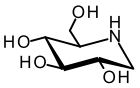

1-deoxynojirimycin (DNJ)

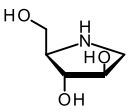

1,4-dideoxy-1,4-imino-D-arabinitol (DAB)

Fig. 2 Miyazaki et al.

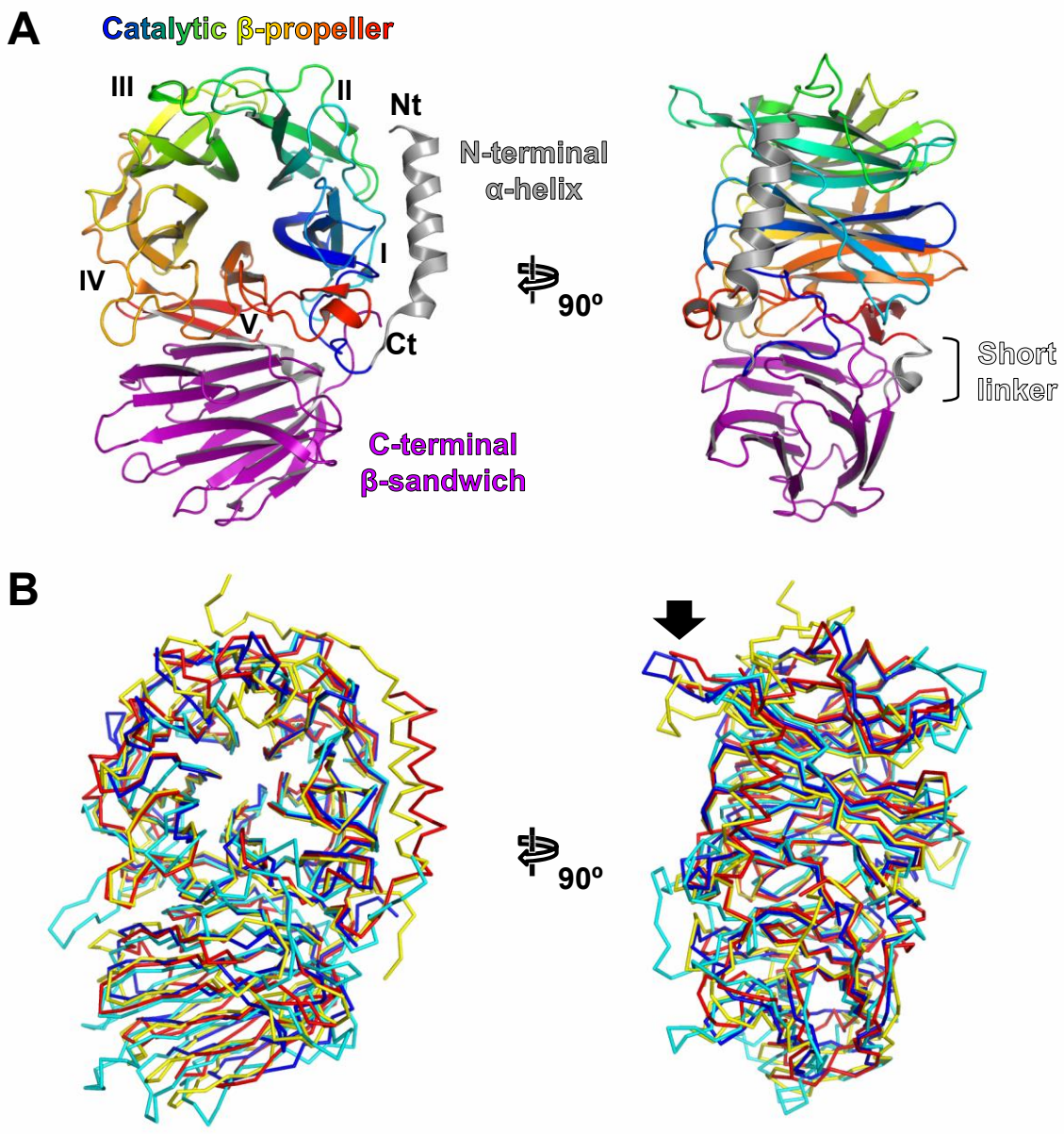

Fig. 3 Miyazaki et al.

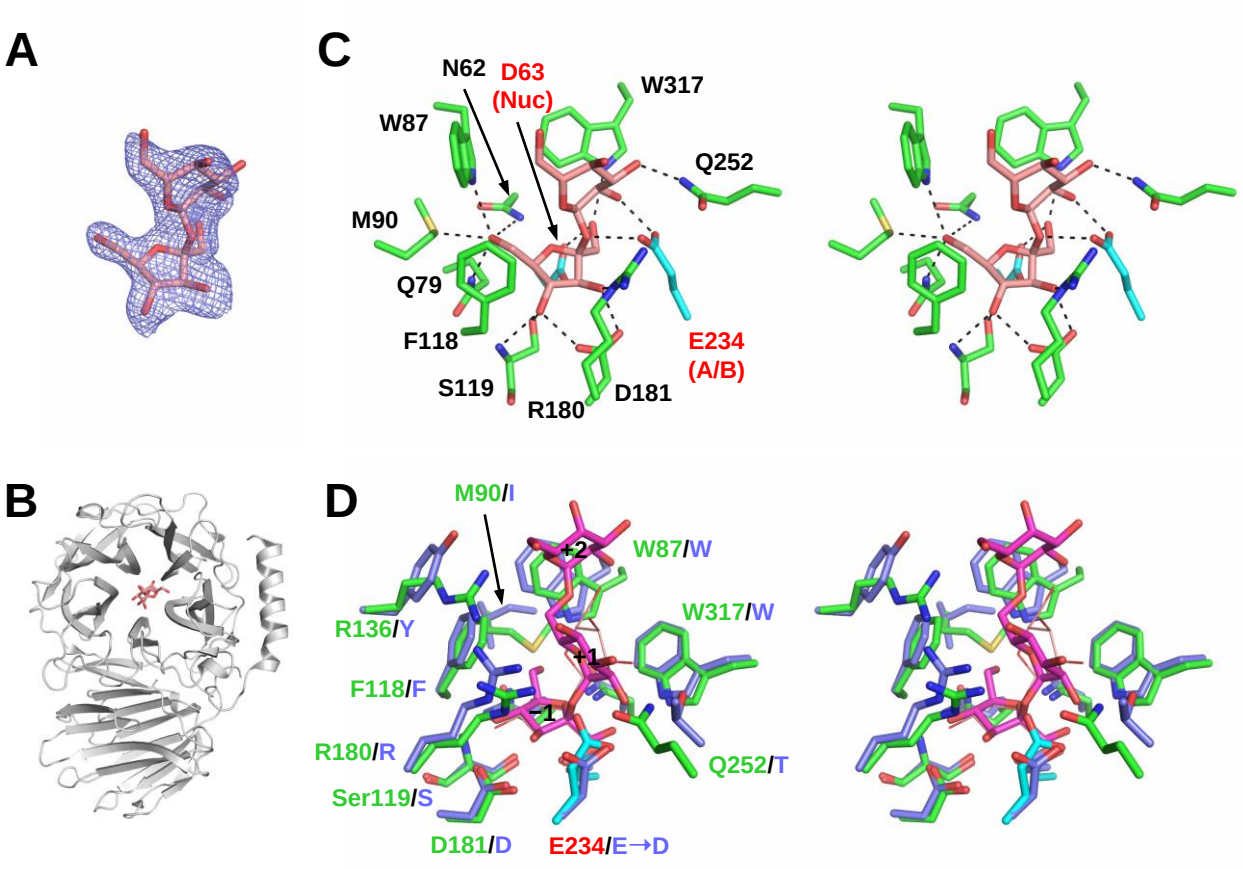

Fig. 4 Miyazaki et al.

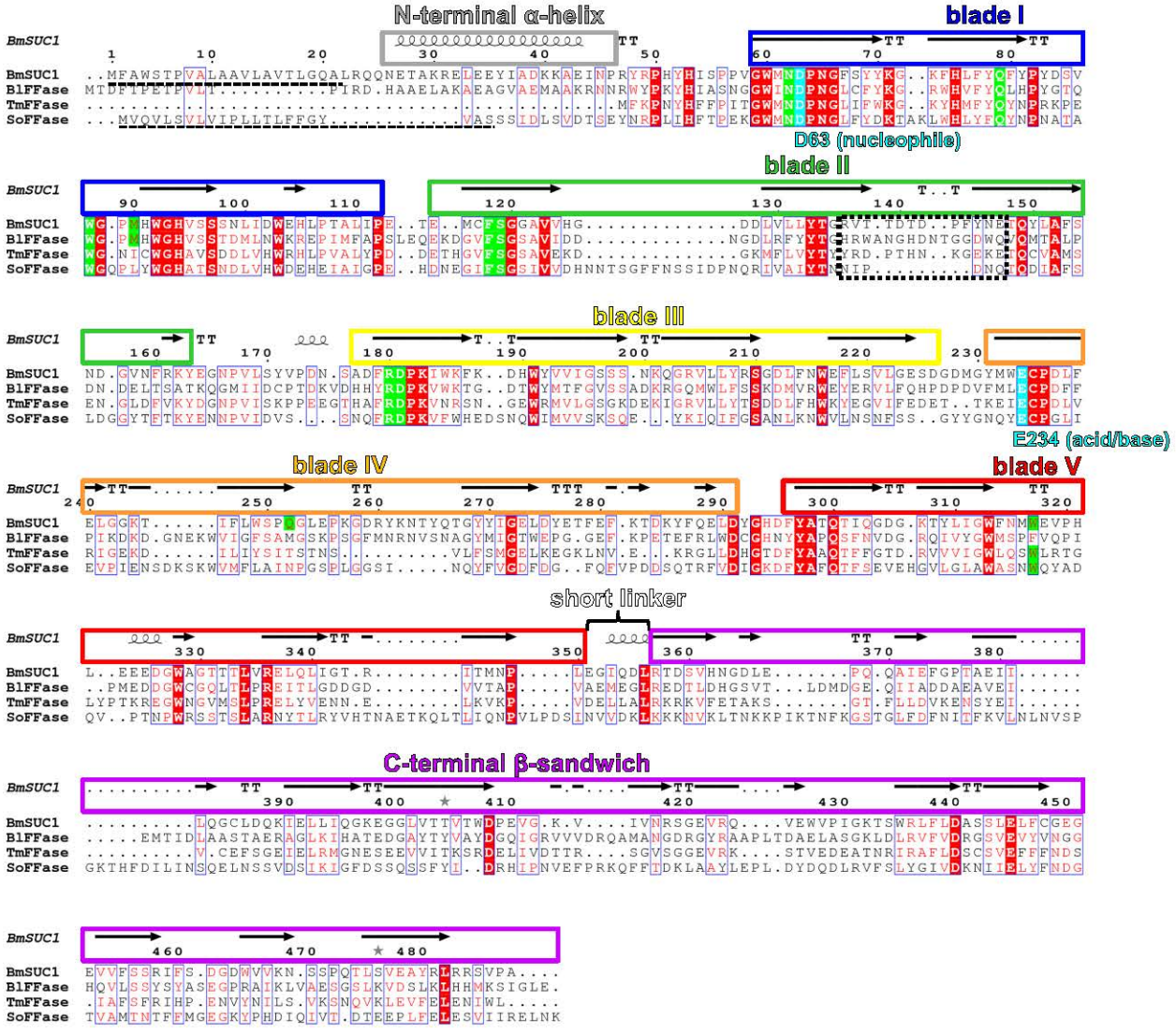

Fig. 5 Miyazaki et al.

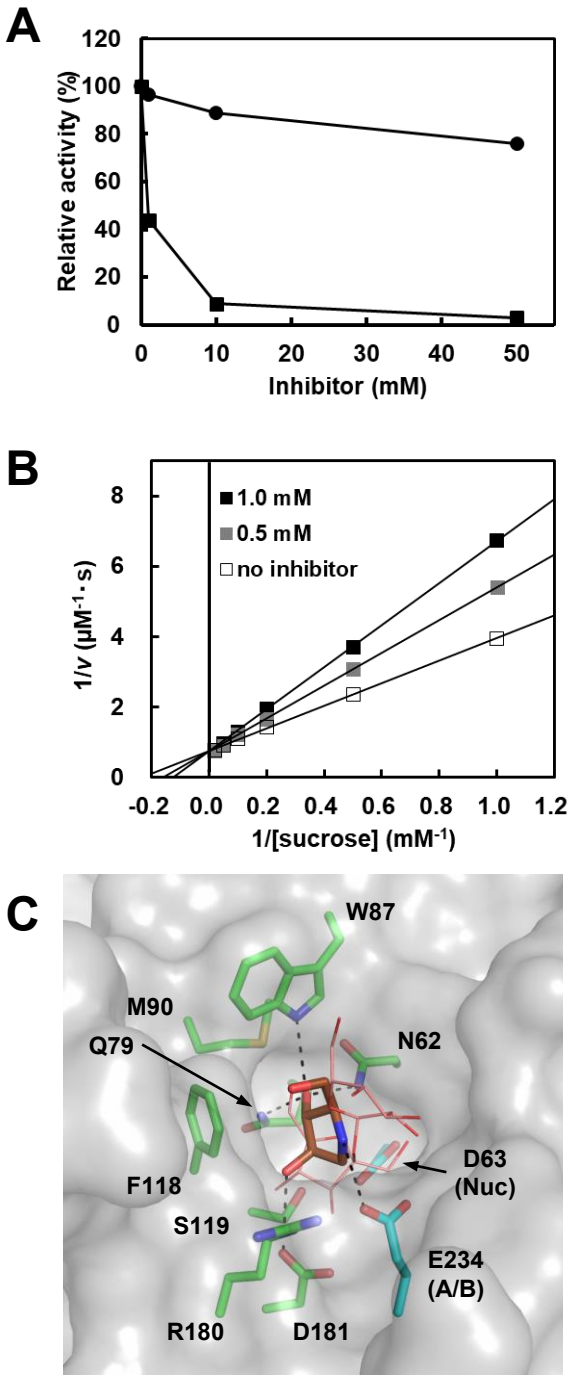

Fig. 6 Miyazaki et al.

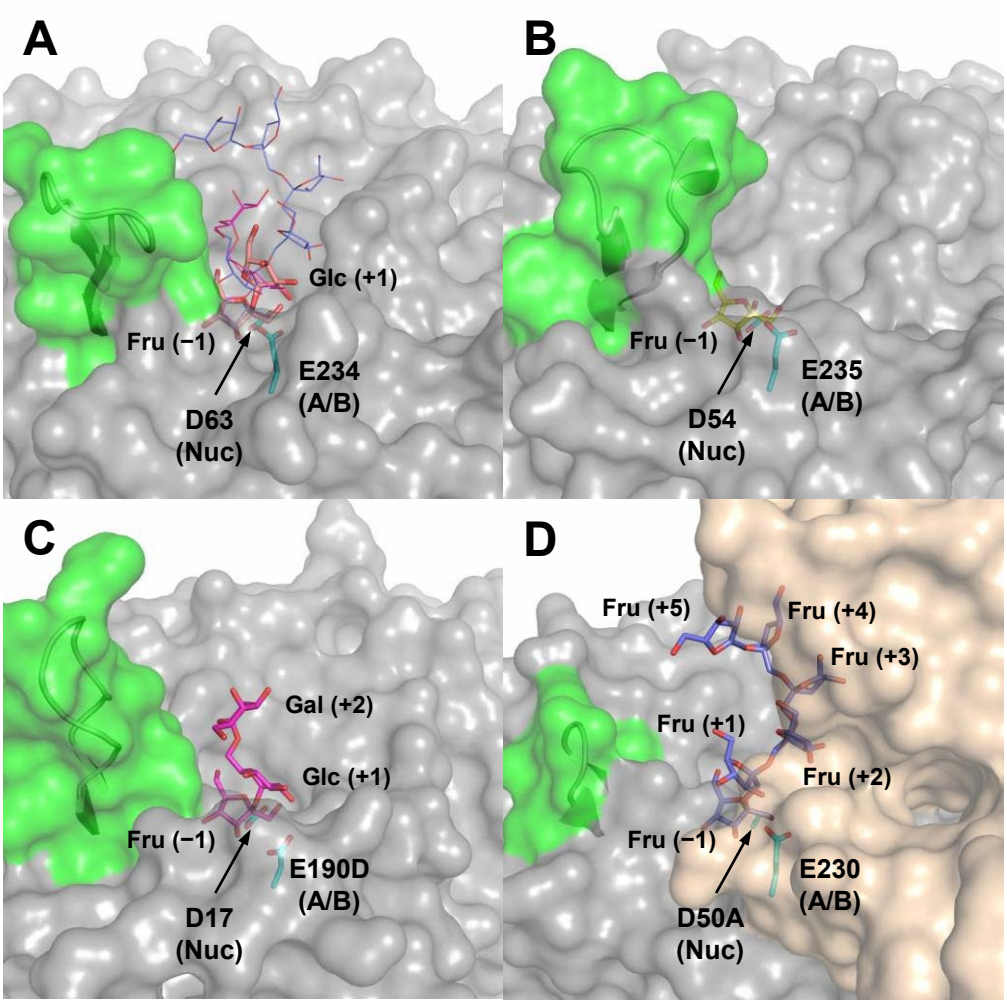

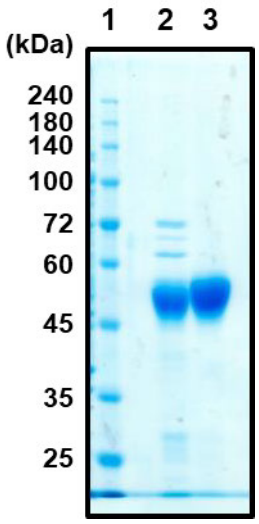

Supplementary Figure S1. SDS-PAGE analysis of the purified recombinant BmSUC1. Proteins were analyzed by SDS-PAGE with a 10% acrylamide gel. Lane 1, ExcelBand All Blue Broad Range Plus Protein Marker (PM1700, SMOBIO Technology, Hsinchu, Taiwan); lane 2, BmSUC1 purified by Ni-NTA affinity chromatography; lane 3, BmSUC1 further purified by gel filtration chromatography.

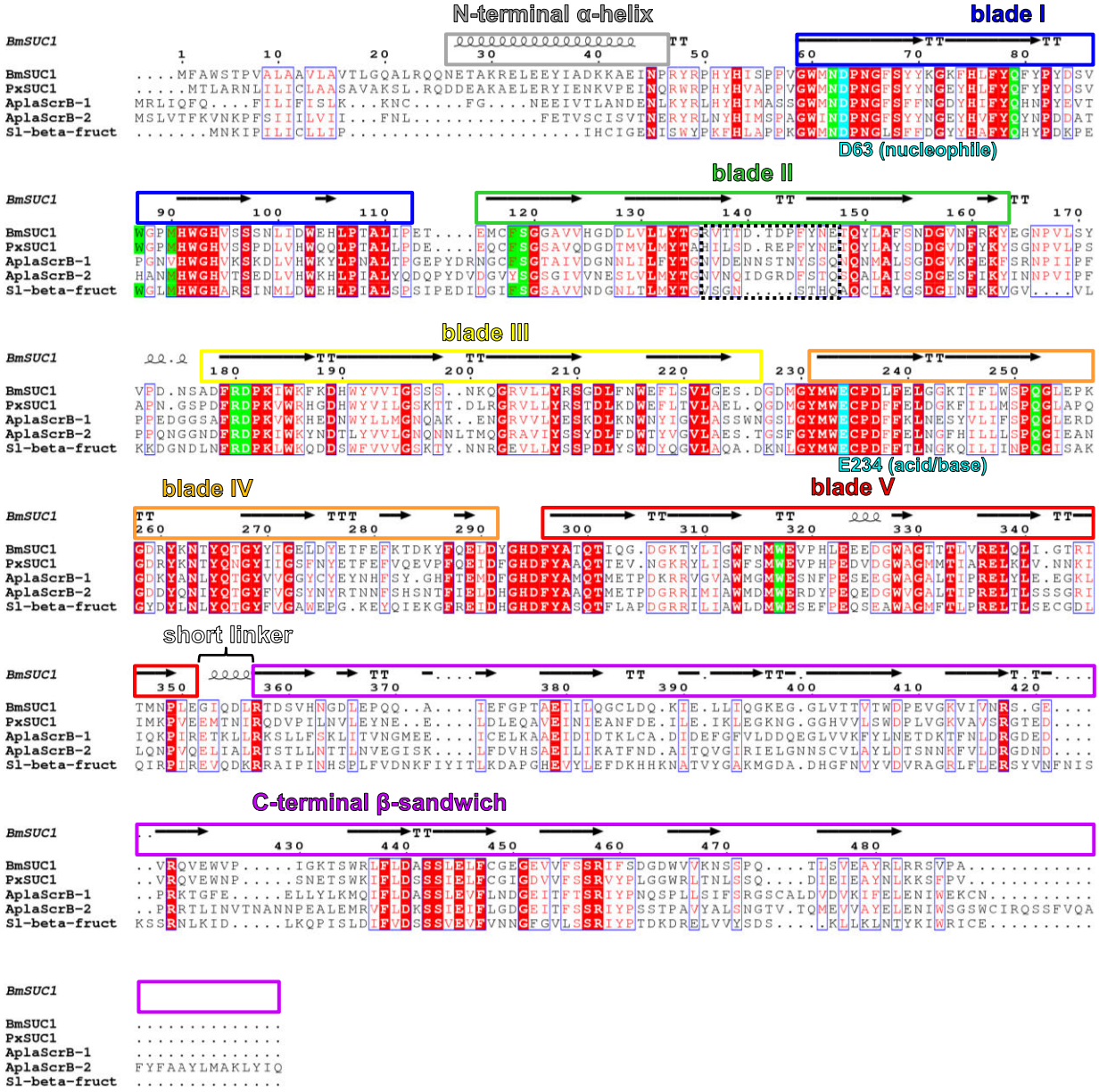

Supplementary Figure S2. Multiple sequence alignment of insect GH32 proteins. The sequences of BmSUC1 and *Papilio xuthus* GH32 ortholog (PxSUC1, GenBank KPJ02556.1, amino acid sequence identity to BmSUC1 = 57.4%), *Agrilus planipennis* β-fructofuranosidase 1 (AplaScrB-1, AIR93897.1, 38.2%), *A. planipennis* β-fructofuranosidase 2 (AplaScrB-2, AIR93898.1, 41.9%), and *Sphenophorus levis* β-fructofuranosidase (Sl-β-fruct, AIL92341.1, 37.9%) were aligned using Clustal Omega and the figure generated by ESPript 3.0. Secondary structures and domain architecture of BmSUC1 are described above sequences and colors for the domains are the same as Fig. 2A. Loop-A and the corresponding regions are boxed with dotted lines. The catalytic residues and residues interacting with sucrose in BmSUC1 are highlighted in cyan and green, respectively. Their identical residues in the other β-fructofuranosidases are also highlighted in the same colors.

Supplementary Table S1. Distances of hydrogen bonds between BmSUC1 and sucrose in the crystal structure of D63A in complex with sucrose.

Sucrose atom	Protein atom	Distance (Å)
Fru −1		
O1	Asp63 OD1 (superimposed)	2.6
	Trp317 NE1	3.1
O2 (glycosidic O)	Glu234 OE2	2.8
O3	Arg180 NE	2.9
	Asp181 OD2	2.5
O4	Ser119 N	2.8
	Ser119 OG	3.0
	Asp181 OD1	2.6
O6	Asn62 ND2	3.3
	Gln79 NE2	2.4
	Trp87 NE1	3.0
	Met90 SD	3.1
Glc +1		
O2	Glu234 OE1	2.7
O3	Gln252 NE2	2.6